

## Effect of Number and Location of Amine Groups on the Thermodynamic Parameters on the Acridine Derivatives to DNA

Ji Hye Kwon, Hee-Jin Park, Nataraj Chitrapriya, Sung Wook Han,<sup>†</sup> Gil Jun Lee,<sup>†,\*</sup> Dong Jin Lee,<sup>‡</sup> and Tae-Sub Cho<sup>\*</sup>

Department of Chemistry, Yeungnam University, Gyeong-buk 712-749, Korea. \*E-mail: tscho@yu.ac.kr

<sup>†</sup>School of Herb Medicine Resource, Kyungwoon University, Gyeong-buk 730-852, Korea. \*E-mail: leegiljun@hanmail.net

<sup>‡</sup>Department of Chemical Engineering, Kyungil University, Gyeong-buk 712-701, Korea

Received October 30, 2012, Accepted December 11, 2012

The thermodynamic parameters for the intercalative interaction of structurally related well known intercalators, 9-aminoacridine (9AA) and proflavine (PF) were determined by means of fluorescence quenching study. The fluorescence intensity of 9AA decreased upon intercalation to DNA, poly[d(A-T)<sub>2</sub>] and poly[d(G-C)<sub>2</sub>]. A van't Hoff plot was constructed from the temperature-dependence of slope of the ratio of the fluorophore in the absence and presence of a quencher molecule with respect to the quencher concentration, which is known as a Stern-Volmer plot. Consequently, the thermodynamic parameters, enthalpy and entropy change, for complex formation was calculated from the slope and y-intercept of the van't Hoff plot. The detailed thermodynamic profile has been elucidated the exothermic nature of complex formation. The complex formation of 9AA with DNA, poly[d(A-T)<sub>2</sub>] and poly[d(G-C)<sub>2</sub>] was energetically favorable with a similar negative Gibb's free energy. On the other hand, the entropy change appeared to be unfavorable for 9AA-poly[d(G-C)<sub>2</sub>] complex formation, which was in contrast to that observed with native DNA and poly[d(A-T)<sub>2</sub>] cases. The equilibrium constant for the intercalation of PF to poly[d(G-C)<sub>2</sub>] was larger than that to DNA, and was the largest among sets tested despite the most unfavorable entropy change, which was compensated for by the largest favorable enthalpy. The favorable hydrogen bond contribution to the formation of the complexes was revealed from the analyzed thermodynamic data.

**Key Words :** 9-Aminoacridine, Proflavine, Intercalation, Thermodynamics

### Introduction

Lerman originally explained the intercalative binding mode, in which an intercalating molecule is sandwiched between two adjacent base pairs<sup>1</sup> and the molecular plane of intercalator is parallel with the base pairs of nucleic acid. Upon intercalation, the DNA-helix elongates by 34 nm per molecule corresponding to the van der Waals thickness of the aromatic intercalator as a consequence the DNA helix unwinding. Interestingly, the essential biological functions, such as transcription, replication and DNA repair could be disturbed by means of structural changes in DNA molecule. This phenomenon is an important indicator of the bioactivity of drugs (ligands). For these causes, intercalators can be used as antiseptics and antitumor drugs.<sup>2,3</sup> Intercalators for duplex DNA, such as ethidium bromide (EB),<sup>4,5</sup> benzo(e)-pyridoindole (BePI),<sup>6</sup> 9-aminoacridine (9AA, Fig. 1)<sup>7,8</sup> and their derivatives, can stabilize the duplex. In order to understand the nature of intercalators and intercalation process, several theoretical and experimental studies have been carried on the thermodynamic stability of intercalated complexes.<sup>9-13</sup> In general, the intercalation process is as follows: first, the drug approaches DNA and binds the outside of DNA; and second, the drug intercalates the DNA base pairs *via* a hydrophobic interaction and forms a stable intercalated complex. The hydrophobic interaction is the major intermolecular interaction in the intercalation. The stability of the inter-

calated complex is related to  $\pi$ -stacking interactions between the intercalator and nucleobase pairs of DNA. Carbon and hydrogen atoms in the intercalator have relatively high electron densities that will exhibit energetically favorable  $\pi$ -stacking interactions with the DNA base pairs.<sup>12,14-17</sup> Thermodynamic parameters, specifically enthalpy, free energy and entropy, reveal the forces that drive complex formation and mechanism of action. 9-Aminoacridine and proflavine (denoted as PF) (Fig. 1), which are polycyclic aromatic compounds with a heterocyclic nitrogen atom, are a useful molecules because of their potential as chemotherapeutic agents<sup>2,18</sup> and probes in molecular biology.<sup>19</sup> These molecules are known as intercalators and interact with double stranded DNA and RNA *via* intercalation.<sup>20-24</sup> Our aim is to scrutinize the thermodynamic stability of 9AA and PF intercalated in DNA base pairs. As shown in Figure 1, the molecular struc-

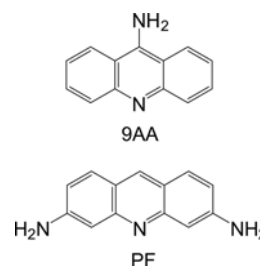


**Figure 1.** Molecular structure of 9-aminoacridine (9AA) and proflavine (PF).

ture of 9AA and PF has a different number of amine groups and located at the different places. The importance of the number and position of amine groups in acridine moiety in the stabilization of intercalated complexes would be firmly explained as a result of thermodynamic investigation.

### Materials and Methods

**Materials.** 9-AA and PF were purchased from Sigma Aldrich and used as received. *Calf thymus* DNA (refer to DNA), poly[d(G-C)<sub>2</sub>] and poly[d(A-T)<sub>2</sub>] (Sigma Aldrich) were dissolved in a buffer containing 100 mM NaCl, 5 mM cacodylate and 1 mM EDTA at pH 7 by constant stirring at 4 °C. The DNA solution was dialyzed five times at 5 h intervals against the 5 mM cacodylic buffer with 100 mM NaCl at 4 °C. The concentrations of the chemicals and DNA were determined spectrophotometrically using the molar extinction coefficients:  $\epsilon_{258\text{nm}} = 6,700 \text{ M}^{-1}\text{cm}^{-1}$  for DNA,  $\epsilon_{254\text{nm}} = 8,400 \text{ M}^{-1}\text{cm}^{-1}$  for poly[d(G-C)<sub>2</sub>],  $\epsilon_{262\text{nm}} = 6,600 \text{ M}^{-1}\text{cm}^{-1}$  for poly[d(A-T)<sub>2</sub>],  $\epsilon_{400\text{nm}} = 9,300 \text{ M}^{-1}\text{cm}^{-1}$  for 9AA and  $\epsilon_{444\text{nm}} = 42,000 \text{ M}^{-1}\text{cm}^{-1}$  for PF. The absorption spectra of the samples were recorded on a Shimadzu UV-1601PC spectrophotometer.

**Fluorescence Quenching.** Fluorescence quenching is a process in which the fluorescence intensity of a given fluorophore decreases after adding a quencher. It has been well documented that there are two types of the quenching mechanism: static and collisional (or dynamic) quenching. In general, fluorescence quenching occurs through one of the two mechanisms or a combination of both. Both mechanisms can be described using the Stern-Volmer equation.<sup>25</sup>

$$\frac{F_0}{F} = 1 + K_{SV}[Q] \quad (1)$$

where  $F$  and  $F_0$  are the fluorescence intensities in the presence and absence of a quencher, respectively, and  $[Q]$  denotes the concentration of the quencher, *i.e.* DNA in this study. In the above equation,  $K_{SV}$  is the Stern-Volmer constant, which is the product of the collisional rate constant and fluorescence life time of the quencher for the dynamic quenching mechanism. For the static mechanism, where the fluorophore loses its fluorescence by forming a non-fluorescent complex with the quencher,  $K_{SV}$  denotes the association constant for the formation of a non-fluorescent complex between the fluorophore and quencher. The fluorescence spectra were measured using a Perkin-Elmer LSB50B spectrofluorometer. The emission spectrum of 9AA and PF were measured using an excitation wavelength of 430 nm and 444 nm, respectively, with slit widths of 5/5 nm for both excitation and emission. The temperature was maintained within  $\pm 0.5$  °C using a water circulating system.

### Results and Discussions

**Spectroscopic Characteristics of 9AA and PF Complexed with DNA and Polynucleotide.** Hypochromism and red

shift are normally observed due to the strong interactions between the aromatic chromospheres of the ligand and the base pairs of the double strand DNA. A spectral change of 9AA and PF with addition of DNA and various polynucleotides is shown in Figure 2. The absorption spectrum of DNA, poly[d(G-C)<sub>2</sub>] and poly[d(A-T)<sub>2</sub>] were subtracted from those of the corresponding complex for sake of easy comparison. The 9AA showed an absorption spectrum in the region of 350-450 nm with vibration structures at 363, 382, 401 and 422 nm. On addition of DNA, poly[d(G-C)<sub>2</sub>] or poly[d(A-T)<sub>2</sub>], the absorption spectrum shows hypochromism of  $\sim 50\%$  with red shift of 7-8 nm in the maximal peak at 401 nm, which is characteristic of the typical intercalative binding mode. The extensive hypochromicity accompanied by red shift in the absorption maxima revealed the strength of an intercalative binding, as previously reported.<sup>20-22</sup> Alternatively, PF exhibited a featureless broad absorption band centered at 444 nm and it was hypochromially shifted by ca. 11.2%, along with the larger red shift (16 nm in  $\lambda_{\text{max}}$ , from 444 to 460 nm.) compared to 9AA upon binding to DNA. Hence, the spectral feature of PF is comparable to the previ-

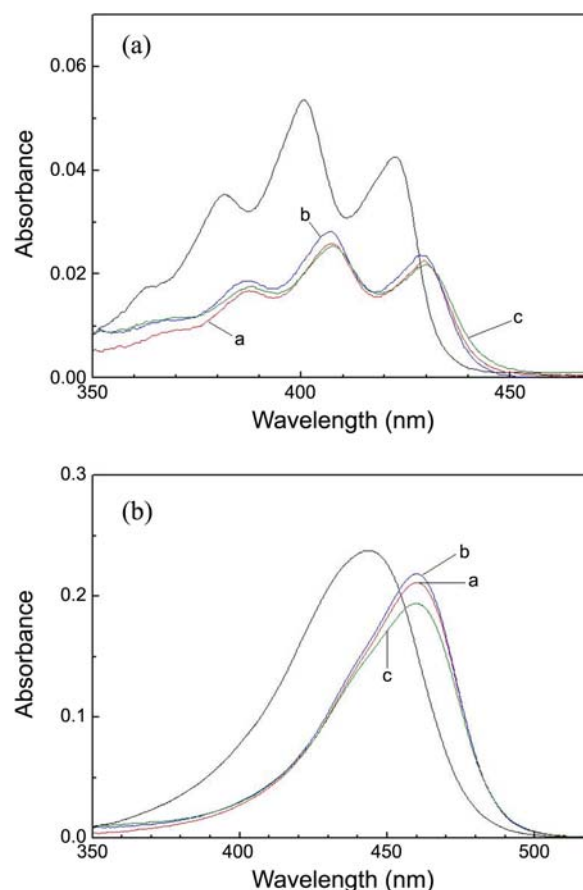


**Figure 2.** Absorption spectra of 9AA (panel a) and PF (panel b) in the absence and presence of DNA, poly[d(A-T)<sub>2</sub>] and poly[d(G-C)<sub>2</sub>]. In panel b, the black curve denotes the absorption spectrum of PF in the absence of DNA, and curves a (red), b (blue) and c (green) represent the absorption spectrum of PF complexed with DNA, poly[d(A-T)<sub>2</sub>] and poly[d(G-C)<sub>2</sub>], respectively. [DNA] = 1 mM, [9AA] = [PF] = 50  $\mu\text{M}$ . Path length = 1 mm.

ous reports.<sup>23,24</sup> In the presence of the synthetic polynucleotides, the identical red shift in the absorption maximum occurred with apparently different hypochromism 7.9% and 17.8% for poly[d(A-T)<sub>2</sub>] and poly[d(G-C)<sub>2</sub>], respectively. The spectral changes that we observed (hypochromicity and red shift) for the 9AA and PF are differed only slightly from each other, indicating that their interactions with DNA were similar, and also it was likely that these compounds may bind to the helix by intercalation.

Figure 3(a) and 3(b) represents the fluorescence emission spectra of 9AA and PF in the absence and presence of polynucleotides, respectively. The results showed that the fluorescence intensity of 9AA decreased with the addition of the DNA or synthetic polynucleotides, which indicated that the 9AA could interact to DNA and polynucleotides in the similar manner. The 9AA is located in a different environment in the presence poly[d(A-T)<sub>2</sub>] than DNA and poly[d(G-C)<sub>2</sub>] since smearing in the vibration bands was observed for the 9AA-poly[d(A-T)<sub>2</sub>] complex. Under this experimental conditions, the quantum yield of 9AA estimated from the area under the emission spectrum decreased to 36.3%, 18.7% and 38.1% upon binding to DNA, poly[d(G-C)<sub>2</sub>] and poly[d(A-

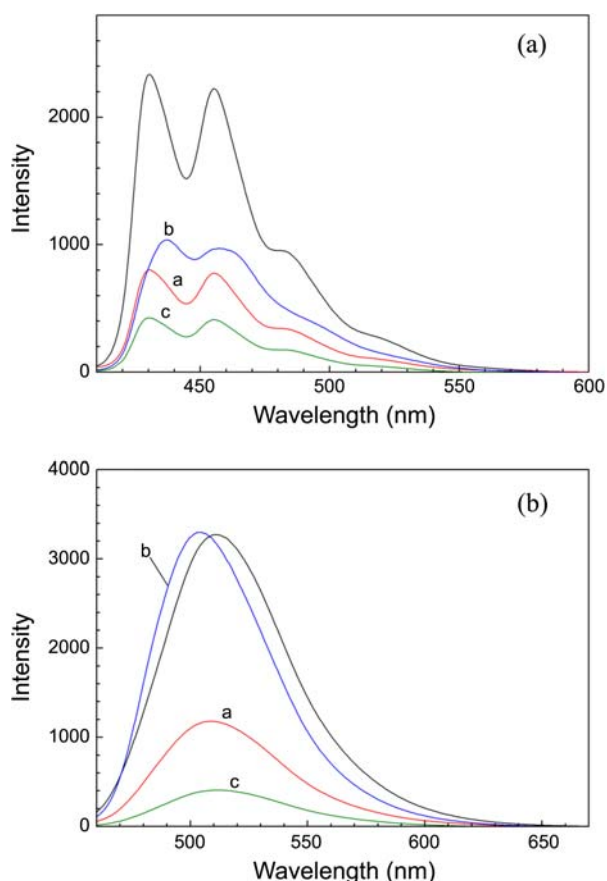


**Figure 3.** Changes in the fluorescence emission spectra of (a) 9AA and (b) PF in the presence of DNA and synthetic polynucleotides. Curve a: DNA; curve b: poly[d(A-T)<sub>2</sub>] and curve c: poly[d(G-C)<sub>2</sub>]. The black curve denotes the emission spectrum in the absence of DNA. The excitation wavelength was 400 nm and 444 nm for 9AA and PF, respectively. [9AA] = [PF] = 2 μM, [DNA] = 50 μM. The slit widths were 5/5nm for both excitation and emission.

T)<sub>2</sub>], respectively. Similarly, the addition of DNA and poly[d(G-C)<sub>2</sub>] in to PF led to a significant decrease of emission intensity, while it increased upon formation of a complex with poly[d(A-T)<sub>2</sub>]. Although PF has been reported to intercalate between DNA base-pairs, and pattern of change in absorption spectrum of PF bound to poly[d(A-T)<sub>2</sub>] resembles with those to DNA and poly[d(G-C)<sub>2</sub>] (Fig. 2), difference in emission spectrum suggested that environment surrounding PF is different in a large extent in poly[d(G-C)<sub>2</sub>] and poly[d(A-T)<sub>2</sub>]. Thus, the measurement of the equilibrium constant using the fluorescence quenching was not applicable for the PF-poly[d(A-T)<sub>2</sub>] complex formation.

**Fluorescence Quenching.** In order to determine the fluorescence quenching mechanism, the fluorescence quenching data at different temperatures (10-50 °C) were analyzed using the classical Stern-Volmer equation. The Stern Volmer plots of 9AA and PF at two representative temperatures (10 and 50 °C) are shown in Figures 4(a) and (b). The value of the fluorescence quenching was linear over a wide concentration range of DNA. Moreover, the similar straight lines obtained

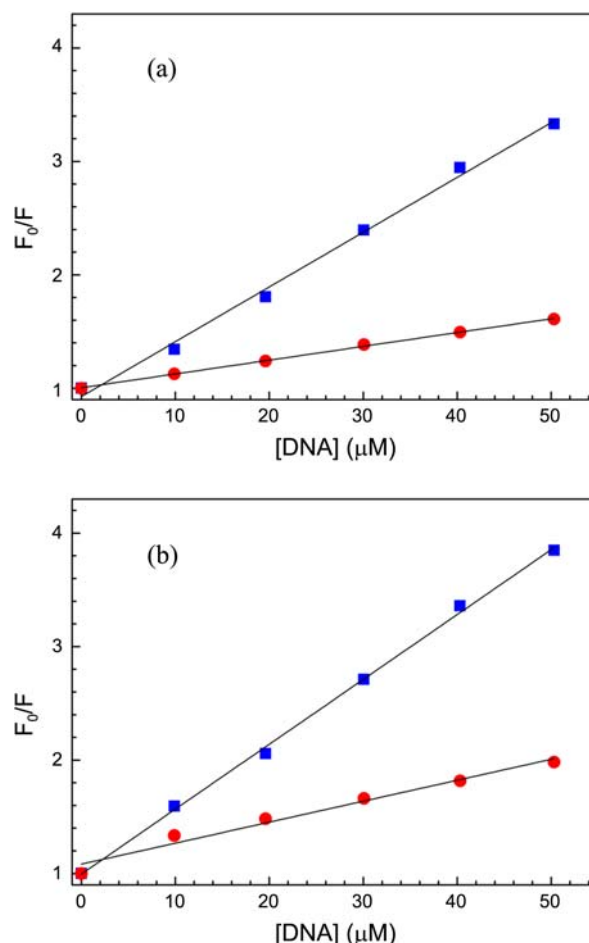


**Figure 4.** Stern-Volmer plot for complex formation of (a) 9AA and (b) PF with DNA at two representative temperatures namely, 10 °C (blue squares) and 50 °C (red circles). The curves measured at intermediate temperatures (20, 30 and 40 °C) were between these two extremes. The fluorescence emission intensities were measured at 400 nm and 444 nm for 9AA and PF, respectively. [9AA] = [PF] = 2 μM.

at temperatures between these two extremes and those are positioned in between these two lines. A straight line in the Stern-Volmer plot suggests that the mechanism behind observed fluorescence quenching is either a simple static or a dynamic-collisional quenching process.<sup>25</sup> Dynamic and static quenching can be distinguished by their differing dependence on temperature and excited-state lifetime. Since the dynamic quenching is due to the diffusion, the quenching efficiency should be increased with increasing temperature. On the contrary, increased temperature is likely to result in decreased quenching efficiency in the static quenching process if the complex formation is an exothermic process, which is the case for most drug-DNA complex formation. As shown in Figure 4 the quenching efficiencies of both 9AA and PF decreased with increasing in temperature thereby indicating the presence of static quenching. Therefore, as discussed in the experimental section, the Stern-Volmer constant,  $K_{SV}$ , can be considered the equilibrium constant for complex formation. It is not possible to compare the equilibrium constant where the fluorescence intensity increases with the formation of the complex. Therefore, the equilibrium constant is not determined for PF-poly[d(A-T)<sub>2</sub>] case and will not be discussed anymore. Table 1 summarizes the calculated equilibrium constants from Stern-Volmer plots at 20 °C. The 9AA-poly[d(G-C)<sub>2</sub>], 9AA-poly[d(A-T)<sub>2</sub>] and PF-poly[d(G-C)<sub>2</sub>] complexes exhibited also similar trend in the fluorescence quenching responses to that observed in 9AA- and PF-DNA complexes.

#### Thermodynamics Parameters for Complex Formation.

Indeed, the thermodynamic parameters of DNA-drug complex are crucial for a scrupulous understanding of the driving forces prevailing the binding of drugs to DNA. The thermodynamic parameters of the 9AA and PF with various DNA can be attained from the following basic thermodynamic equations by using equilibrium constants at various temperatures.

$$\ln K_{SV} = -\frac{\Delta H^0}{RT} + \frac{\Delta S^0}{T} \quad (2)$$

$$\Delta G^0 = -RT \ln K_{SV} \quad (3)$$

where  $\Delta H^0$  is the standard change of enthalpy,  $\Delta S^0$  is the standard change of entropy and  $\Delta G^0$  is the standard change in Gibbs free energy for the formation of a drug-DNA complex.  $R$  is the gas constant and  $T$  is the temperature in Kelvin. Using Eq. (2),  $\Delta H^0$  and  $\Delta S^0$  can be calculated from the slope and  $y$ -intercept of the plot of  $\ln K_{SV}$  vs.  $1/T$ , which is known as the van't Hoff plot. Figure 5 shows the van't Hoff plots for 9AA and PF-DNA, in which the equilibrium constants were obtained from the fluorescence quenching experiment. On the whole, the hydrogen bonding between the bound drugs and DNA, van der Waals stacking interaction, hydrophobic interaction force, arrangement of the hydration molecules in the drugs and DNA spine and steric contacts are plays an vital role to interpret the thermodynamic stability of the complex formation. The calculated thermodynamic parameters including entropy and enthalpy change of complex

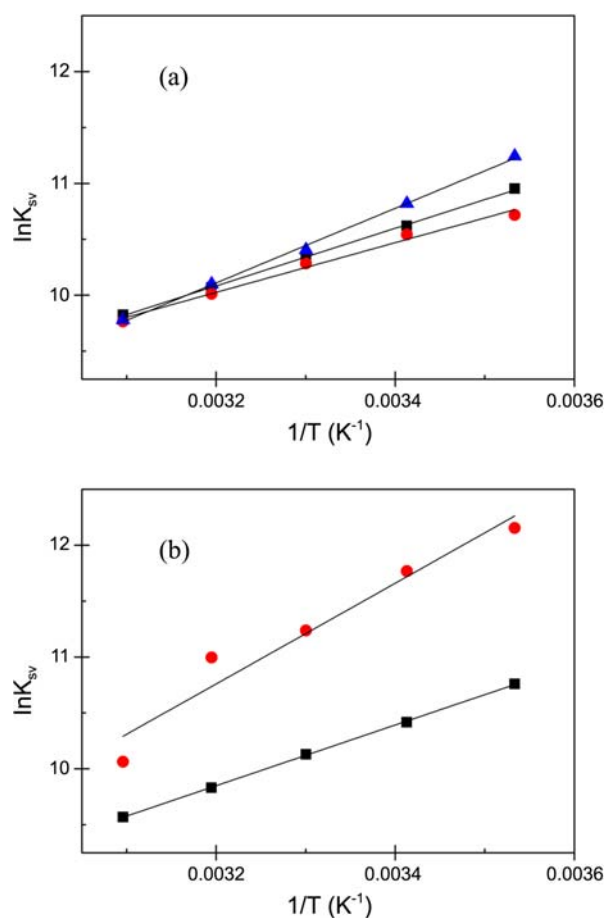


**Figure 5.** Van't Hoff plot for the complex formation of (a) 9AA and (b) PF with poly[d(A-T)<sub>2</sub>] (blue triangles), poly[d(G-C)<sub>2</sub>] (red circles) and DNA (black squares). In the PF case, addition of poly[d(A-T)<sub>2</sub>] did not result in the fluorescence quenching hence, the quenching method described in this work was not applicable.

formation at 20 °C are summarized in Table 1. It is clearly observed from the experimental results that the complex formation for all the cases was spontaneous with similar negative  $\Delta G^0$  values. From the negative values of  $\Delta G^0$ , it has been revealed that the complex formation is exothermically driven process with a large negative value of the standard

**Table 1.** Thermodynamic parameters for the complex formation between 9AA and PF with DNA and synthetic polynucleotides

	$K, M^{-1}$	$\Delta H^0,$ kJ·mol <sup>-1</sup>	$\Delta S^0,$ J·K <sup>-1</sup> ·mol <sup>-1</sup>	$\Delta G^0,$ kJ·mol <sup>-1</sup>
9-Aminoacridine				
DNA	$4.10 \times 10^4$	-21.39	15.40	-25.90
Poly[d(G-C) <sub>2</sub> ]	$5.00 \times 10^4$	-27.79	-4.86	-26.37
Poly[d(A-T) <sub>2</sub> ]	$3.79 \times 10^4$	-18.46	24.27	-25.57
Proflavine				
DNA	$3.34 \times 10^4$	-22.56	9.67	-25.40
Poly[d(G-C) <sub>2</sub> ]	$12.9 \times 10^4$	-37.44	-30.36	-28.54

The equilibrium constant and the Gibbs free energies represent those at 20 °C.

change in enthalpy, which signifies the energy difference between the product and reactant. In particular, a favorable enthalpy change was noted in the case of PF-poly[d(G-C)<sub>2</sub>] complex formation. The standard change in entropy, which means the change in the degree of disorder in the process of complex formation, was either positive (favorable) or negative (unfavorable). As per the thermodynamic data, the formation of 9AA- and PF-poly[d(G-C)<sub>2</sub>] complexes are entropy disfavored, indicating that the complex formed with poly[d(G-C)<sub>2</sub>] is more ordered than their dissociated state. It has been established that the strong interaction between a DNA-bound drug and stacking interaction between DNA bases and the planar aromatic part of the drug as indicated by large negative enthalpy changes. The negative enthalpy ( $\Delta H$ ) value illustrates that hydrogen bonding forces most likely play an essential role in the stabilization of the complex. These interactions should be large enough to compensate for the interactions between the solution and drug, and between the solution and DNA. Stacking between the DNA bases and intercalated drug as well as the formation of hydrogen bonds result unfavorable entropy for complex formation. Consequently, the entropy of the system will be decreased by distortion of the DNA base pairs where drug insertion and the release of the solvation shell originally surrounding the drug and DNA. Thus, the observed effects in entropy and enthalpy for the intercalation of 9AA and PF may perhaps the combination of these interactions. It is noteworthy that the complex formation of PF with poly[d(G-C)<sub>2</sub>] far more enthalpically favorable with an almost four times higher equilibrium constant than formation PF-DNA complex. In the case of PF complex, the observed favorable enthalpy was compensated for by the large unfavorable entropy. This can be explained by the formation of hydrogen bonds that include the amine groups protruding in the minor grooves of DNA. It should be noted that the 9AA also has observed similar consequence on complex formation, but to a less extent. Although the significantly higher favorable enthalpy and negative  $\Delta G^0$  values obtained for 9AA and PF is quite similar, decrease in entropy of 9AA complexes compensated for the largely favorable enthalpy. The increase in negative enthalpy and negative entropy were far more pronounced for PF than 9AA-poly[d(G-C)<sub>2</sub>] complexation. It clearly shows formation of hydrogen bonds between PF and the GC base-pairs may be more effective or the number of hydrogen bonds for PF is larger compared to 9AA. Although the binding mode of 9AA toward DNA and synthetic polynucleotides is similar to that of PF, little dissimilarity has been observed for their thermodynamic stability of the complex formation.

### Conclusions

The intercalation of 9AA and PF to DNA, poly[d(G-C)<sub>2</sub>]

and poly[d(A-T)<sub>2</sub>] are energetically favorable with a negative Gibb's free energy. The equilibrium constant for the intercalation of 9AA to poly[d(G-C)<sub>2</sub>] was larger than that to DNA and poly[d(A-T)<sub>2</sub>]. PF also exhibited a larger equilibrium constant when intercalated to poly[d(G-C)<sub>2</sub>] compared to DNA. These higher equilibrium constants might be due to the formation of a larger number of hydrogen bonds.

**Acknowledgments.** This study was supported by an internal research grant of Yeungnam University.

### References

- Lerman, L. S. *J. Mol. Biol.* **1961**, *3*, 18.
- Brana, M. F.; Cacho, M.; Gradillas, A.; Pascuala-Teresa, B.; Bomos, A. *Curr. Phar. Design.* **2001**, *7*, 1745.
- Li, S.; Cooper, V. R.; Thonhauser, T.; Lundqvist, B. L.; Langreth, D. L. *J. Phys. Chem. B* **2009**, *113*, 11166.
- Denny, W. A. *Curr. Med. Chem.* **2002**, *9*, 1655.
- Topal, M. D. *Biochemistry* **1981**, *23*, 2367.
- Hansen, J. B.; Koch, T.; Buchardt, O.; Nielsen, P. E.; Wirth, M.; Nordén, B. *Biochemistry* **1983**, *22*, 4878.
- Kim, H. K.; Cho, T. S.; Kim, S. K. *Bull. Korean Chem. Soc.* **1996**, *17*, 358.
- Schelhorn, T.; Kretz, S.; Zimmermann, H. W. *Cell Mol. Biol.* **1992**, *38*, 345.
- Sacria, P. V.; Shafer, R. H. *J. Biol. Chem.* **1991**, *266*, 5417.
- Tuite, E.; Nordén, B. *Bioorg. Med. Chem.* **1995**, *3*, 701.
- Pilch, D. S.; Martin, M. T.; Nguyen, C. H.; Sun, J. S.; Bisagni, E.; Monternary-Garestier, T.; Hélène, C. *J. Am. Chem. Soc.* **1993**, *232*, 926.
- Kim, H. K.; Kim, J. M.; Kim, S. K.; Rodger, A.; Nordén, B. *Biochemistry* **1992**, *31*, 10671.
- Hyun, K. M.; Lee, G. J.; Cho, T. S.; Kim, S. K.; Yi, S. Y. *Bull. Korean Chem. Soc.* **1997**, *18*, 528.
- Řeha, D.; Kabeláč, M.; Ryjáček, F.; Šponer, J.; Šponer, J. E.; Elstner, M.; Suhai, S.; Hobza, P. *J. Am. Chem. Soc.* **2002**, *124*, 3366.
- Mukherjee, A.; Lavery, R.; Bagchi, B.; Hynes, T. *J. Am. Chem. Soc.* **2008**, *130*, 9747.
- Dymant, L. N.; Veselkov, A. N. *Theo. and Experi. Chem.* **1993**, *28*, 329.
- Nafisi, S.; Saboury, A. A.; Keramat, N.; Neault, J.-F.; Tajmir-Riahi, H.-A. *J. Mol. Struct.* **2007**, *827*, 35.
- Kano, K.; Baba, Y.; Kagemoto, A.; Beatty, L. *Poly. J.* **1983**, *15*, 657.
- Řeha, D.; Kabelac, M.; Ryjacek, F.; Sponer, J. E.; Elstner, M.; Suhai, S.; Hobza, P. *J. Am. Chem. Soc.* **2002**, *124*, 3366.
- Hunter, C. A.; Lawson, K. R.; Perkins, J.; Urch, C. J. *J. Chem. Soc. Perkin Trans.* **2001**, *2*, 651.
- Patterson, S. E.; Coxon, J. M.; Strekowski, L. *Bioorg. Med. Chem.* **1997**, *5*, 277.
- Giacomoni, P. U.; Le Bret, M. *FEBS Lett.* **1973**, *29*, 227.
- Aslanoglu, M. *Anal. Sci.* **2006**, *22*, 439.
- García, B.; Leal, J. M.; Ruiz, R.; Biver, T.; Secco, F.; Venturini, M. *J. Phys. Chem. B* **2010**, *114*, 8555.
- Lakowiz, J. R. In *Principles of Fluorescence Spectroscopy*; Plenum Publisher: New York, 2001; p 237.